

# Real-Time Obstacle Avoidance by Visually Recognizing Laser Patterns<sup>\*</sup>

Wen-Chung Chang<sup>\*</sup> Chih-Wei Cho<sup>\*\*</sup>

<sup>\*</sup> Department of Electrical Engineering, National Taipei University of Technology, Taipei, Taiwan, R. O. C. Email: wchang@ee.ntut.edu.tw

<sup>\*\*</sup> Department of Electrical Engineering, National Taipei University of Technology, Taipei, Taiwan, R. O. C. Email: chihwei.cho@gmail.com

---

**Abstract:** This paper presents a 3-D local map building approach for real-time obstacle avoidance using visually-recognized laser patterns. Precise estimate of the local map provides essential information for navigation and control of a mobile robot in unknown environments. Existing navigation and control approaches typically require expensive sensing devices, such as sonar or laser range finder. In this paper, a mobile robot mounted with a CCD camera and a laser line projector is proposed for the considered control tasks. The idea is to reconstruct the actively-projected laser line in Cartesian space from its observed image based on known geometrical relation between the laser line projector and the CCD camera. The position of the obstacle can thus be estimated based on the reconstructed laser line for effective and efficient navigation of mobile robot. The proposed system has been effectively validated in laboratory environments by performing experiments with a custom-made wheeled robot.

---

## 1. INTRODUCTION

Recently, research on mobile robots has been extensively applied in a variety of environments such as offices, factories, and hospitals. Therefore, mobile robots have to be equipped with a number of sensing devices to navigate in real environments in a safe way. In order to perform required tasks while avoiding obstacles, a number of sensors such as laser range finders, ultrasonic sensors, stereo-camera-based range sensors are typically employed. Vision is becoming a popular sensor for robot control since it can extract extensive information without contacting with the environment. It can also imitate human eyes to complete a variety of tasks [Chang, 2006, 2007a,b] with precision.

Visual simultaneous localization and map building (V-SLAM) problem asks if it is possible for an autonomous vehicle to start in an unknown location in an unknown environment and then to incrementally build a map of this environment based on vision sensors while simultaneously using this map to compute absolute vehicle location. V-SLAM has been studied by many researchers using different structure. The approaches employing stereo vision [Kim and Kim, 2004, Se et al., 2005] is one of the main streams. But, it is well known that the stereo vision approach is very time-consuming and must deal with the correspondence problem. There are also different approaches employing single-camera vision. Ulrich and Nourbakhsh [2000] proposed a robot navigation method to avoid obstacles by searching obstacles using visual clues such as color, texture and edge. Jeong and Lee [2006] used line and corner features to accomplish the map building and the required control task. Nguyen et al. [2006] proposed a simple landmark model for localization and

<sup>\*</sup> This research was supported by the National Science Council of Taiwan, R.O.C. under grants NSC 94-2213-E-027-006 and NSC 96-2752-E-027-002-PAE.

mapping of mobile robots. Although these methods could reduce redundant computation and also avoid correspondence problem, these methods still need prior knowledge about the environments to complete localization and map building. What this paper is concerned is to accomplish real-time obstacle avoidance based on 3-D local map building that is fast and efficient. Moreover, this seemingly novel approach can be further integrated to resolve V-SLAM problems.

In this research, a mobile robotic system employing a CCD camera and a laser projector is capable of building local obstacle maps for real-time robot navigation. The proposed system could successfully detect the laser line patterns actively projected on surrounding obstacles and identify them in Hough space. Given the geometrical relation between the camera and the laser projector, the laser patterns can be reconstructed in Cartesian space to build the 3-D local map for robot navigation without prior knowledge about the environment. Meanwhile, compared with existing approaches, the novel approach appears to be simple, low-cost, and effective. The paper is organized as follows. Section 2 briefly describes the proposed robotic system. Section 3 presents the way to detect laser patterns and target point in image space. The reconstruction of laser patterns in Cartesian space are illustrated in Section 4. Section 5 introduces the control law for obstacle avoidance. Section 6 reports experimental results validating effectiveness of the proposed system. Finally, concluding remarks are addressed in Section 7.

## 2. SYSTEM DESCRIPTION

This paper presents a local map building approach which enables a custom-made wheeled robot to navigate in unknown environments. The proposed approach can detect obstacles based on a single CCD camera and a laser line

projector to build local maps of obstacles in Cartesian space. The control goal is to drive a mobile robot to a target point in an unknown environment while avoiding collision with any possible obstacles. The robot first detects the laser patterns, actively projected by the laser line projector, in the image plane. Then, the positions of the laser patterns in Cartesian space are reconstructed based on calibrated geometrical relation between the laser line projector and the CCD camera. The local obstacle maps in Cartesian space can thus be built accordingly. Finally, the mobile robot is controlled to a target point while avoiding collision with surrounding obstacles by temporarily diverting its heading. The structure of the proposed obstacle avoidance system is shown in Fig. 1.

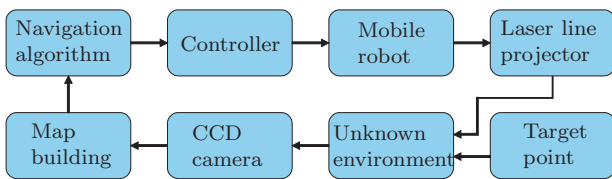


Fig. 1. Structure of the proposed obstacle avoidance system.

### 3. LASER LINE AND TARGET POINT DETECTION

To know where any obstacle is, the robot projects a laser line on it and then process the image observed by the CCD camera. To detect the laser pattern on an obstacle, typical thresholding in RGB color space is performed as follows.

$$240 > R > 180 \quad (1)$$

$$100 > G > 70 \quad (2)$$

$$100 > B > 70 \quad (3)$$

After detecting the laser pattern on the image plane, the robot needs to identify it as a line or a set of points in image space for further reconstruction in 3-D space. In order to determine equation of the line easily, Hough transform [Woods, 2003, Chang and Lee, 2004] is employed. Each line can be determined in the Hough space by estimating its parameters as illustrated in Fig. 2. Specifically, a line in image space can be represented by

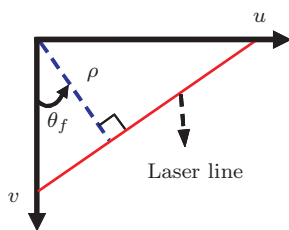


Fig. 2. Illustration of Hough parameters in image plane.

$$v \cos \theta_f + u \sin \theta_f = \rho \quad (4)$$

where  $v$  is the vertical coordinate on the image,  $u$  is the horizontal coordinate on the image,  $\rho$  is the vertical distance from the origin to the laser line in image space,

and  $\theta_f$  is the angle between  $\rho$  and  $v$ . When the laser pattern projected on the obstacle can not be identified as a complete line in image space, each identified image point is reconstructed in 3-D space directly. Therefore, the proposed system can work under simple and complicated environments. Typical detection results can be seen in the left image of Fig. 3, where the identified laser pattern is shown in blue color. Similarly, the target point marked

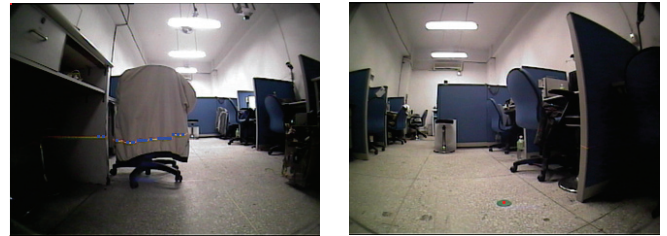


Fig. 3. Typical detection and thresholding result of laser pattern (left) and target (right).

by color labels can be detected by color filtering and connected components labeling. A typical observed target point image from a CCD camera and the corresponding image processing results can be seen in the right image of Fig. 3, where the green circle is the target and the red point is the detected target center.

### 4. RECONSTRUCTION OF LASER LINE

In an unknown environment, roadway and obstacles are highly important for navigation of a mobile robot. Therefore, their 3-D positions are the most critical for local map building. Based on the detected laser pattern, the position of the projected laser pattern in Cartesian space can be reconstructed by calibrated CCD and laser line projector system. Specifically, one can compute the intersecting point of the laser plane and the ray that starts from the optical center of the laser projector and passes the corresponding laser point in image plane. The schematic diagram illustrating the proposed approach is shown in Fig. 4. Based on the aforementioned method, the positions

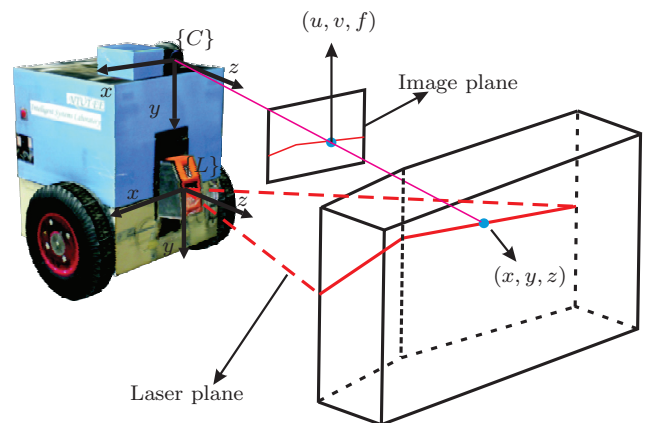


Fig. 4. Camera-Laser system diagram.

of all laser points, a line or a set of points, in Cartesian space can be reconstructed. The detail of the reconstruction method is listed as follows. Firstly, coordinate systems

$C$  and  $L$  are attached at the optical centers of the CCD camera and the laser line projector respectively. Frame  $L$  is relative to frame  $C$  by the following mapping.

$${}^C \mathbf{p} = {}^C_L \mathbf{R} {}^L \mathbf{p} + {}^C \mathbf{p}_{LORG} \quad (5)$$

where  ${}^C_L \mathbf{R}$  is the rotation matrix and  ${}^C \mathbf{p}_{LORG}$  is the translation vector. Since the laser projector is fixed under the camera with tilt motion, the rotation matrix and translation vector can be defined based on the known geometrical relation between the camera and the laser projector as follows.

$${}^C_L \mathbf{R} = \begin{bmatrix} 1 & 0 & 0 \\ 0 & \cos \alpha & \sin \alpha \\ 0 & -\sin \alpha & \cos \alpha \end{bmatrix} \quad (6)$$

$${}^C \mathbf{p}_{LORG} = [0 \ d \ 0]^T \quad (7)$$

where  $d$  is the distance between the optical centers of the camera and the laser projector and  $\alpha$  is the angle of rotation of frame  $L$  relative to frame  $C$  around  ${}^L \mathbf{x}$ .

Select two linearly independent vectors  ${}^L \mathbf{w}_1$  and  ${}^L \mathbf{w}_2$  which span the laser plane. For example, one can select three non-collinear points on the laser plane such as  $[0 \ 0 \ 0]^T$ ,  $[1 \ 0 \ 0]^T$ , and  $[0 \ 0 \ 1]^T$  when the tilt angle  $\alpha$  is zero. The two vectors  ${}^L \mathbf{w}_1$  and  ${}^L \mathbf{w}_2$  can thus be defined as

$${}^L \mathbf{w}_1 = [0 \ \sin \alpha \ \cos \alpha]^T \quad (8)$$

$${}^L \mathbf{w}_2 = [1 \ 0 \ 0]^T. \quad (9)$$

Based on these two vectors, the normal vector to the laser plane can be calculated based on the cross product of these two vectors.

$${}^C \mathbf{n} = {}^L \mathbf{w}_1 \times {}^L \mathbf{w}_2 = [0 \ -\cos \alpha \ \sin \alpha]^T \quad (10)$$

Therefore, the laser plane can be described in the camera frame by

$${}^C \mathbf{n} \cdot {}^C \mathbf{p} = k \quad (11)$$

In the light of the fact that the laser plane passes the optical center of the laser projector, one can set that

$$k = {}^C \mathbf{n} \cdot {}^C \mathbf{p}_{LORG} = -d \cos \alpha \quad (12)$$

Therefore, the laser plane described in the camera frame is

$${}^C \mathbf{n} \cdot {}^C \mathbf{p} = -d \cos \alpha \quad (13)$$

or

$$-y \cos \alpha + z \sin \alpha = -d \cos \alpha \quad (14)$$

Based on the image geometry, the position of any terminal point in Cartesian space and the image plane must satisfy the following formula.

$$\frac{x}{u} = \frac{y}{v} = \frac{z}{f} \quad (15)$$

where  $(x, y, z)$  is the coordinate of a terminal point in Cartesian space, and  $(u, v)$  is the coordinate in the image plane, and  $f$  is the focal length of the CCD camera. Based on equations (14) and (15), the position of the laser point in Cartesian space can then be reconstructed as

$$x = \frac{u \cdot (y - d)}{f \cdot \tan \alpha} \quad (16)$$

$$y = \frac{v \cdot (y - d)}{f \cdot \tan \alpha} \quad (17)$$

$$z = \frac{(y - d)}{\tan \alpha}. \quad (18)$$

Therefore, any image point on the laser pattern can be transformed to 3-D space using equations (16)-(18). The proposed sensing architecture appears to be simple and effective. It is based on the concept of 3-D reconstruction employing stereo vision. Certainly, the system is capable of reconstructing laser patterns as long as the baseline, from the optical center of the CCD camera to the center of the laser projector, is not degenerated. To illustrate the idea, the proposed sensing system is tested in a laboratory environment as shown in Fig. 5, where one can see the detection and reconstruction result. The optical center of the CCD camera is located at  $(0, 0)$ , the length between two terminal points is the width of the obstacle.

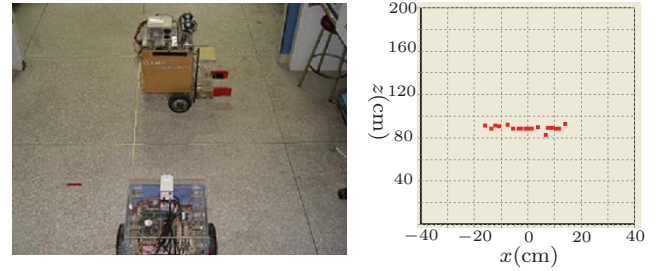


Fig. 5. Detection and reconstruction result in a laboratory environment.

## 5. NAVIGATION AND CONTROLLER DESIGN

The control task is to drive a mobile robot to locate and reach a target point with color labels in an unknown environment while avoiding collision with any possible obstacles during maneuvering. An obstacle avoidance criterion is proposed to effectively prevent the mobile robot from colliding with any obstacle in unknown environments. In particular, if obstacles are located in front of the mobile robot, decision on the moving direction can be made based on the sizes of the robot and the obstacles using the proposed CCD camera and laser line projector system. The complete navigation and control system is illustrated in Fig. 6, where the obstacle avoidance criterion can be seen in Table 1. In Fig. 7, a schematic diagram for obstacle avoidance criterion is shown, where the robot is assumed to be capable of observing both obstacles at same time. If the real boundaries of the obstacles are not within the camera's field of view, the parameters  $d_{l,2}$ ,  $d_{r,1}$  are calculated based on what the vision system can observe on the image plane.

### 5.1 Kinematic model of the mobile robot

The coordinate system is shown in Fig. 8 where The left superscript  $W$  denote the world frame. The pose of the mobile robot is related to the angular velocities of the wheels,  $\omega_L$  and  $\omega_R$ , by

$$\begin{bmatrix} {}^W \dot{x} \\ {}^W \dot{y} \\ \theta \end{bmatrix} = \begin{bmatrix} -\frac{b}{2} \sin \theta & -\frac{b}{2} \sin \theta \\ -\frac{b}{2} \cos \theta & -\frac{b}{2} \cos \theta \\ -\frac{b}{2s} & -\frac{b}{2s} \end{bmatrix} \mathbf{u} \quad (19)$$

$$\mathbf{u} = \begin{bmatrix} \omega_L \\ \omega_R \end{bmatrix} \quad (20)$$

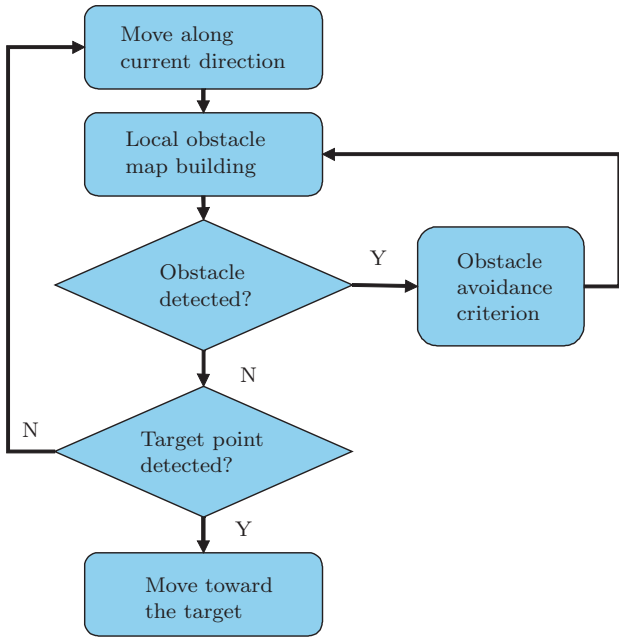


Fig. 6. Flowchart of the proposed navigation and control system.

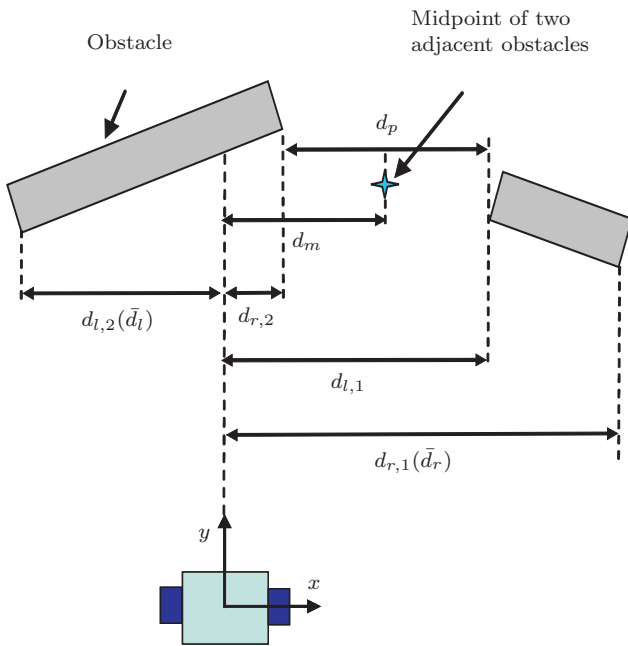


Fig. 7. Schematic diagram for obstacle avoidance criterion.

where  $b$  is the radius of the wheels and  $s$  is half of the distance between two wheels.

### 5.2 Controller design

The mobile robot is required to reach a target while avoiding collision with any obstacle. To do so, the robot needs to accomplish three different motion behaviors. The first one is to alternate the heading by turning left or right to avoid colliding with obstacles, where the control law is defined as

Table 1. Obstacle avoidance criterion

<ul style="list-style-type: none"> <li>Based on the reconstructed local obstacle map, the behavior of the mobile robot can be determined as follows:                      If (there is no obstacle detected or the distance between the robot and the nearest obstacle <math>&gt;</math> a pre-determined safe distance).                      {                          Robot continues moving along current or a pre-determined direction.                      }                      If (obstacles are in front of the robot)                      {                          Calculate the lateral distances <math>d_l</math> and <math>d_r</math> of each obstacle, which is the lateral distance between the robot and the left and right sides of the obstacle respectively.                          Set <math>d_l</math> of the most left obstacle as <math>\bar{d}_l</math> and <math>d_r</math> of the most right obstacle as <math>\bar{d}_r</math>.                          Calculate the lateral distance <math>d_p</math> between each adjacent obstacle pair and the lateral distance <math>d_m</math> between the robot and the midpoint of each adjacent obstacle pair.                          If ((any <math>d_p &gt;</math> robot width) and <math>d_m &lt; \bar{d}_l</math> and <math>d_m &lt; \bar{d}_r</math>)                          {                              Drive the robot to pass through the two adjacent obstacles.                          }                          Else if (<math>\bar{d}_l \geq \bar{d}_r</math>)                          {                              Drive the robot to turn right.                          }                          Else if (<math>\bar{d}_l &lt; \bar{d}_r</math>)                          {                              Drive the robot to turn left.                          }                          }                          Else if (the target point is detected)                          {                              Drive the robot to reach the target.                          }                      }                 </li> </ul>
--

$$\mathbf{u} = \begin{bmatrix} g_1 + \mu g_2 \\ g_1 - \mu g_2 \end{bmatrix} \quad (21)$$

where  $g_1$  and  $g_2$  are appropriate gains and  $\mu$  is either  $-1$  or  $1$  for left or right turn respectively.

The second motion is to drive the mobile robot to pass through two adjacent obstacles. To do so, a virtual target point is set at the middle of the two adjacent obstacles, where the schematic figure illustrating the motion behavior is shown in Fig. 9, where the red dotted line is the actual robot trajectory. The third motion is to control the robot to move toward the target point. The schematic figure for the motion behavior can be seen in Fig. 10, where the red dotted line is the actual robot trajectory and  $d_s$  is a pre-defined distance to ensure the target point is within the camera's field of view. For the set-point tasks required in the second and the third motion behaviors, the control law is defined as follows.



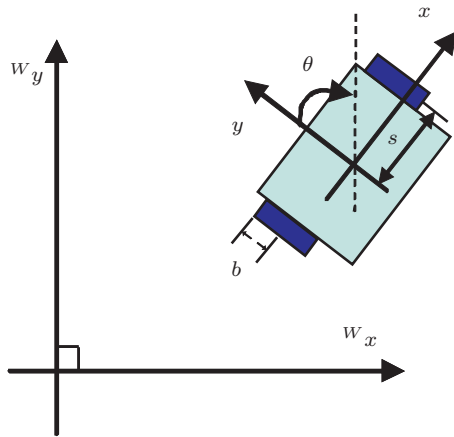


Fig. 8. Coordinate system for the mobile robot.

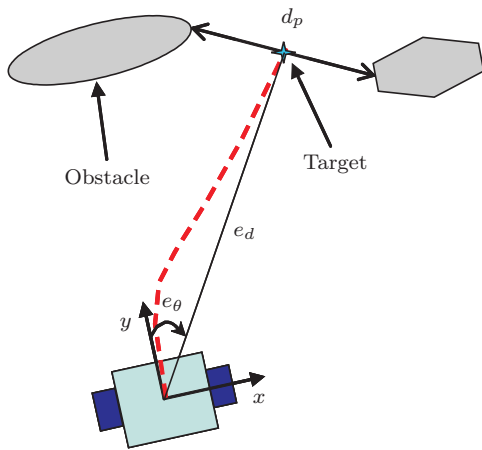


Fig. 9. Schematic diagram for obstacle avoidance.

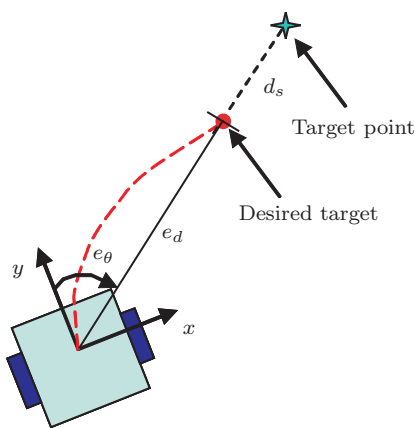


Fig. 10. Schematic diagram for reaching a target.

$$\mathbf{u} = \begin{bmatrix} g_3 \\ g_3 \end{bmatrix} e_d + \begin{bmatrix} -g_4 \\ g_4 \end{bmatrix} e_\theta \quad (22)$$

where  $e_d$  denotes the encoded error of distance,  $e_\theta$  denotes the encoded error of angle, and  $g_3$  and  $g_4$  are appropriately selected control gains.

## 6. EXPERIMENTAL RESULTS

The proposed navigation and obstacle avoidance system has been effectively implemented using a custom-made mobile robot in a real laboratory environment. All image processing and visual servo control computation are performed on an onboard Pentium IV 3.0 GHz PC running Windows XP. The sampling rate of the visual servo control system is around 30 Hz. During the experiments, surrounding obstacles can be efficiently detected by using the onboard laser line projector and CCD camera. The experimental task is to locate and reach a target point while avoiding collision with any obstacle. Typical experimental results are illustrated in Fig. 11, where the red line denotes the robot trajectory. In particular, the controlled motion in this experiment can be performed in three stages once an obstacle is detected at a distance shorter than the pre-determined safe distance.

**Stage 1:** Turn left to avoid colliding with the first obstacle which is another robot.

**Stage 2:** Turn right to avoid colliding with an office chair and continue passing through these two obstacles.

**Stage 3:** Locate and reach the target.

Fig. 12, Fig. 13, and Fig. 14 show the detection and reconstruction results from Stage 1 to 3 respectively.

## 7. CONCLUSION

This paper introduces a seemingly novel sensing architecture for mobile robotic navigation based on visually recognizing actively projected laser patterns. Specifically, the laser pattern is detected and identified in image space by thresholding in RGB color space. Then, it can be reconstructed in Cartesian space based on the calibrated monocular vision and laser line projector system. According to the reconstructed local map, a navigation and control approach is presented for the mobile robot to move toward a target point while avoiding collision with any obstacles. Based on the experimental results, the proposed system appears to be fast, efficient, and effective. The merit of the proposed system is the simple sensing structure that can be applied in unknown environments. Compared with other expensive detection systems, the application of a CCD camera together with a laser projector is much more economical. However, the detection of laser patterns can be further improved in order to assure the robustness of the visually-guided mobile robotic navigation system.

## REFERENCES

- Wen-Chung Chang. Precise positioning of binocular eye-to-hand robotic manipulators. *Journal of Intelligent and Robotic Systems*, 49(3):219–236, July 2007a.
- Wen-Chung Chang. Hybrid force and vision-based contour following of planar robots. *Journal of Intelligent and Robotic Systems*, 47(3):215–237, November 2006.
- Wen-Chung Chang. Binocular vision-based trajectory following for autonomous robotic manipulation. *Robotica*, 25(5):615–626, September 2007b.
- Wen-Chung Chang and Shu-An Lee. Real-time feature-based 3d map reconstruction for stereo visual guidance and control of mobile robots in indoor environments. In *Proc. of the 2004 IEEE International Conference*

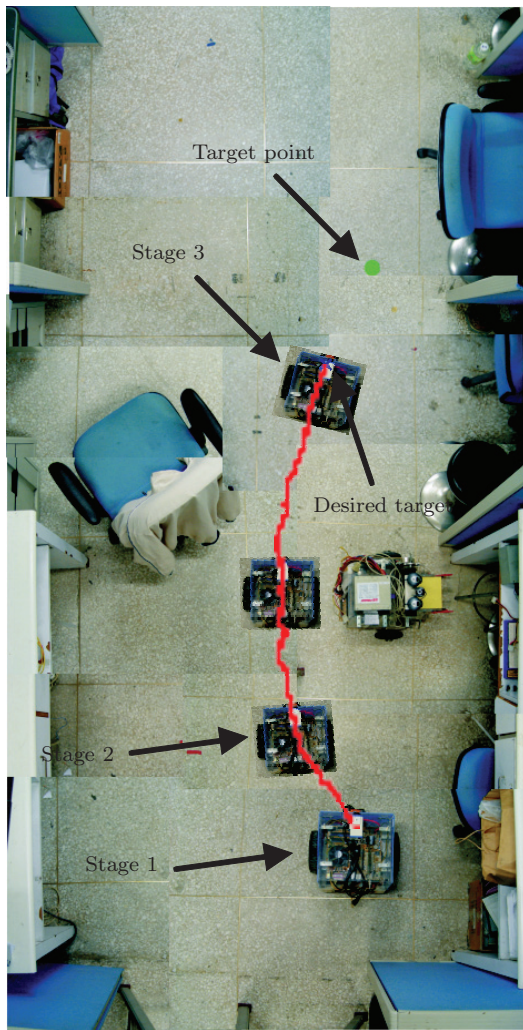


Fig. 11. Bird's eye view of the experimental results.

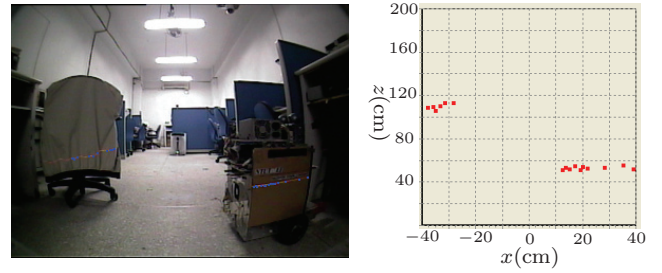


Fig. 13. Detection and reconstruction results at Stage 2.

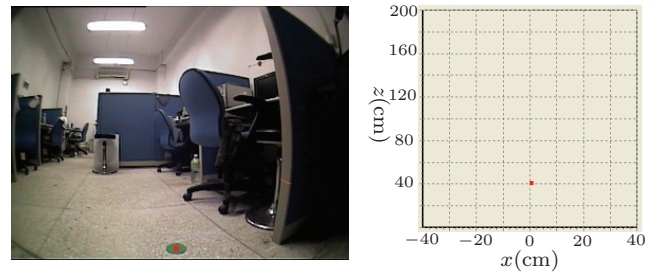


Fig. 14. Detection and reconstruction results at Stage 3.

Xuan-Dao Nguyen, Bum-Jae You, and Sang-Rok Oh. A simple landmark model for vision-based simultaneous localization and mapping. In *Proc. of the IEEE International Joint Conference*, pages 5016–5021, Bexco, Oct 2006.

S. Se, D. G. Lowe, and J. J. Little. Vision-based global localization and mapping for mobile robots. *IEEE Transactions on robotics*, 21(3):364–375, June 2005.

Iwan Ulrich and Illah Nourbakhsh. Appearance-based obstacle detection with monocular color vision. In *Proc. of the AAAI National Conference on Artificial Intelligence*, pages 866–871, Texas, Jul 2000.

R. E. Woods. *Digital Image Processing*. Prentice-Hall, 2003.

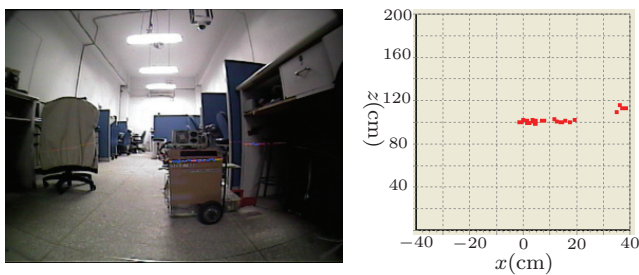


Fig. 12. Detection and reconstruction results at Stage 1.

on *Systems, Man and Cybernetics*, pages 5386–5391, Hague, Netherlands, October 2004. IEEE.

Woo Yeno Jeong and Kyoung Mu Lee. Visual slam with line and corner features. In *Proc. of the IEEE International Conference on Intelligent Robots and Systems*, pages 2570–2575, Beijing, Oct 2006.

Y.-G. Kim and H. Kim. Layered ground floor detection for vision-based mobile robot navigation. In *Proc. of the IEEE International Conference on Robotics and Automation*, pages 13–18, New Orleans, Jan 2004.